A Study on the Ductility of Concrete-Filled Composite Columns under Cyclic Loading

반복하중을 받는 콘크리트충전 강합성 기둥의 연성에 관한 연구

송 준 엽* 권 영 봉** 김 성 곤***
Song, Jun Yeup Kwon, Young Bong Kim, Sung Kon

국문요약

일정한 축하중과 반복적인 횡하중을 받는 콘크리트충전 강합성 기둥의 내진성능에 관한 실험적인 연구가 수행되었다. 강합성 기둥은 충전콘크리트가 강판의 국부좌굴로 인한 내측방향의 변형을 억제하고, 강판의 콘크리트 측압에 대한 구속효과와 같은 상호작용에 의해서 콘크리트와 강재의 단순누가강도 이상의 강도증진효과를 가지며, 강재 및 콘크리트기둥에 비해 우수한 연성 및 에너지 흡수능력을 나타내었다. 단면분할법을 이용하여 콘크리트충전 강합성 기둥의 비선형 모멘트-곡률 관계를 예측해 보았으며, 이는 실험결과와 비교적 잘 일치하는 것으로 나타났다. 또한, 구조물의 내진설계의 중요한 요소인 강합성 기둥의 연성 및 응답수정계수를 평가해 보았다. 실험결과 강합성 기둥은 효과적인 내진구조 부재로 판단되었다.

주요어 : 콘크리트충전 강합성 기둥, 내진설계, 단면분할법, 연성지수, 응답수정계수

ABSTRACT

A series of tests on concrete-filled composite columns was preformed to evaluate structural performance under axial compression and cyclic lateral loading. It was presented that concrete-filled composite columns had high strength, high stiffness and large energy-absorption capacity on account of mutual confinement between the steel plate and filled-in concrete. A cross section analysis procedure developed to predict the moment-curvature relation of composite columns was proven to be an accurate and effective method. The ductility factor and the response modification factor were evaluated for the seismic design of concrete-filled composite columns. It was shown that concrete-filled composite columns could be used as a very efficient earthquake-resistant structural member.

Key words : concrete-filled composite columns, seismic design, cross section analysis, ductility factor, response modification factor

1. Introduction

In recent years, the use of composite columns has widely been increased in the construction of various kinds of structures such as bridge piers of urban highway bridges and light-weight electric railway bridges and columns of high-rise buildings. The concrete-filled composite column has been developed to assure the demands for the strength and deformation capacity in the design of large scale structures. Therefore, extensive researches on the concrete-filled steel box columns have been carried out in the States and Japan since 1980s. The concrete-filled steel columns may have large number of advantages such as large energy-absorption capacity, high impact resistance and enhancement of strength and ductility in comparison with reinforced concrete or steel box columns, since the steel plate can provide sufficient confinement for the in-filled concrete which in turn prevents the inward deformation caused by the local buckling of the steel plate. However, since its strength capacity and earthquake-resistant capacity of composite columns have not been proven clearly, it is necessary to investigate the structural behavior fully for the purpose of seismic design of bridge piers. In this paper, the strength and ductility of the concrete-filled composite columns have been studied with various parameters, such as length of in-filled concrete, number of loading cycles, slenderness ratio and width-thickness ratio, for its application to the bridge pier. Simple and efficient computational procedures for predicting moment-curvature and load-deflection relation and ultimate strength of concrete-filled composite columns have also been developed.

2. Test setup

2.1 Material properties

The tensile coupon test was performed according to KS B 0802 using U.T.M(capacity 250kN) and extensometer to determine the mechanical properties of the steel used and the test results are given in Table 1. The locations of coupons are given in Fig. 1. It was shown that the yield strength of specimens was slightly higher than the nominal yield strength of SS400 but the tensile strength was lower

* 영남대학교 토목도시환경공학부, 강사
** 정회원 · 영남대학교 토목도시환경공학부, 교수(대표저자 : ybkwon@yu.ac.kr)
*** 정회원 · 서울산업대학교 구조공학과, 교수
본 논문에 대한 토의를 2002년 2월 28일까지 학회로 보내 주시면 그 결과를 게재하겠습니다. (논문접수일 : 2001. 7. 13 / 심사종료일 : 2001. 10. 9)

Table 1 Material properties of steel

Specimen No.	F_y (kgf/cm²)	f_u (kgf/cm²)	E_s (kgf/cm²)	F_y/f_u
1	2970	3700	2000000	0.80
2	2860	3760	2040000	0.76
3	2910	3700	2020000	0.79
4	2870	3750	1940000	0.77
Average	2900	3730	2025800	0.78

F_y=yield stress, f_u=ultimate stress, E_s=Young's modulus

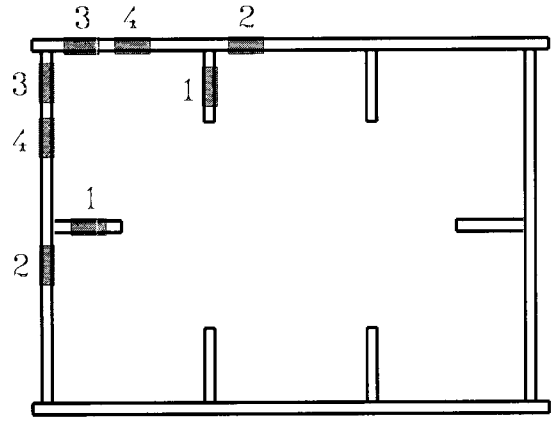

Fig. 1 Locations of tensile coupons

than the nominal strength.

To determine the compressive strength of the concrete, 12 cylinders(10cm diameter×20cm height) were cast from the same batch used inside the concrete-filled column. The cylinders were cured for 28 days before the column specimens and cubes were tested. The average compressive strength of concrete was 250kgf/cm².

2.2 Test specimens

In order to determine the strength and ductility of long composite columns subjected to constant axial load and cyclic lateral load, thirteen concrete-filled steel box columns having width-thickness ratio(R_f), slenderness ratio($\bar{\lambda}$), length of filled-in concrete(l_c) and lateral load history as main test parameters were tested. The variables of width-thickness ratio and slenderness ratio were determined by Eq. (1) and Eq. (2), respectively.

$$R_f = \frac{b}{t}\sqrt{\frac{12(1-\nu^2)}{\pi^2 k}}\sqrt{\frac{F_y}{E_s}} = \sqrt{\frac{F_y}{f_{cr}}} \quad (1)$$

$$\bar{\lambda} = \frac{Kh}{r}\frac{1}{\pi}\sqrt{\frac{f_y}{E_s}} \quad (2)$$

in which, R_f=width-thickness ratio parameter of the flange plate, $\bar{\lambda}$=slenderness ratio parameter of the column, b=flange width, t=plate thickness, F_y=yield stress, E_s=Young's modulus, ν=Poisson's ratio, k=buckling coefficient of a plate($k=4.0n^2$ for a simply supported plate, n=number of sub-panels), K=effective column length factor, h=column height, r=radius of gyration.

For comparison, four long steel box columns were also tested. Detail geometries are shown in Fig. 2 and Table 2. The test setup is shown in Fig. 3 and Fig. 4. Test specimens were designed as cantilever-type columns with relatively small slenderness ratio simulating fixed conditions at the footing and free at the top as in a common practice for designing bridge piers. Concrete was poured from the opening(∅100mm) in the lower end plate up to the specified length where a diaphragm without opening was attached. Since concrete was located between the diaphragm and lower end plate, concrete could be supposed to be in a fully confined state. The concentric axial load applied was 20% of the squash load, P_y, of the test specimens and applied using two tendons tensed by hydraulic jack(capacity 1000kN). The horizontal load was applied by servo controlled hydraulic actuator(capacity 500kN) as shown in Fig. 4.

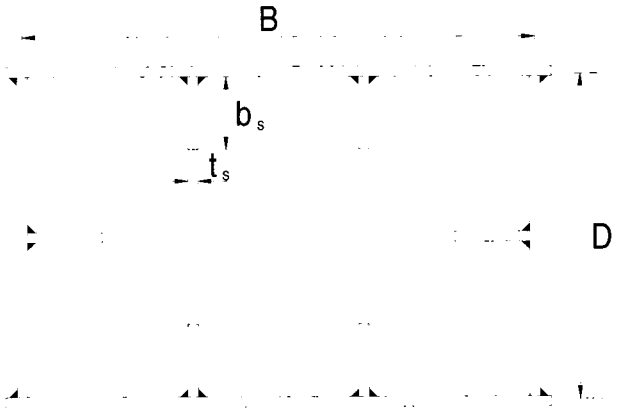

(a) Stiffened section

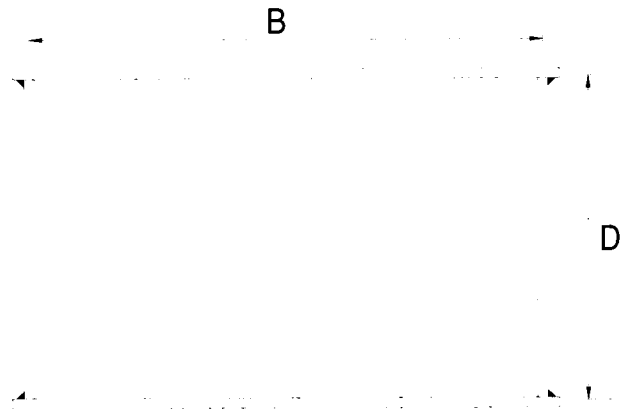

(b) Unstiffened section

Fig. 2 Test specimens

Table 2 Main parameters and dimensions of test specimens(unit : mm)

Specimens	$\bar{\lambda}$	l_c/h	N	P/P_y	B	D	t	t_s	b_s	l_c	L	h
U70-40-0-3	0.42	-	3	0.2	155	125	4	-	-	-	1200	1000
U70-40-3-3	0.42	0.3	3	0.2	155	125	4	-	-	286.5	1200	1000
U70-40-3-0	0.42	0.3	0	0.2	155	125	4	-	-	286.5	1200	1000
U70-60-3-3	0.63	0.3	3	0.2	155	125	4	-	-	286.5	1200	1000
U90-40-0-3	0.43	-	3	0.2	200	160	4	-	-	-	1500	1300
U90-40-3-3	0.43	0.3	3	0.2	200	160	4	-	-	376.5	1500	1300
S40-25-0-3	0.27	-	3	0.2	270	180	4	4	40	-	1100	900
S40-25-3-3	0.27	0.3	3	0.2	270	180	4	4	40	256.5	1100	900
S40-25-5-3	0.27	0.5	3	0.2	270	180	4	4	40	427.5	1100	900
S40-35-3-3	0.36	0.3	3	0.2	270	180	4	4	40	346.5	1400	1200
S40-50-3-3	0.51	0.3	3	0.2	270	180	4	4	40	496.5	1900	1700
S60-25-0-3	0.27	-	3	0.2	396	264	4	4	60	-	1500	1300
S60-25-3-3	0.27	0.3	3	0.2	396	264	4	4	60	376.5	1500	1300
S60-25-5-3	0.27	0.5	3	0.2	396	264	4	4	60	627.5	1500	1300
S60-25-8-3	0.27	0.8	3	0.2	396	264	4	4	60	1004	1500	1300
S60-25-10-3	0.27	1.0	3	0.2	396	264	4	4	60	1255	1500	1300

S 40 25 3 3
- Number of loading cycle
- Length of filled-in concrete
- Slenderness parameter of column
- Width-thickness parameter of flange plate
- U : unstiffened section, S : stiffened section

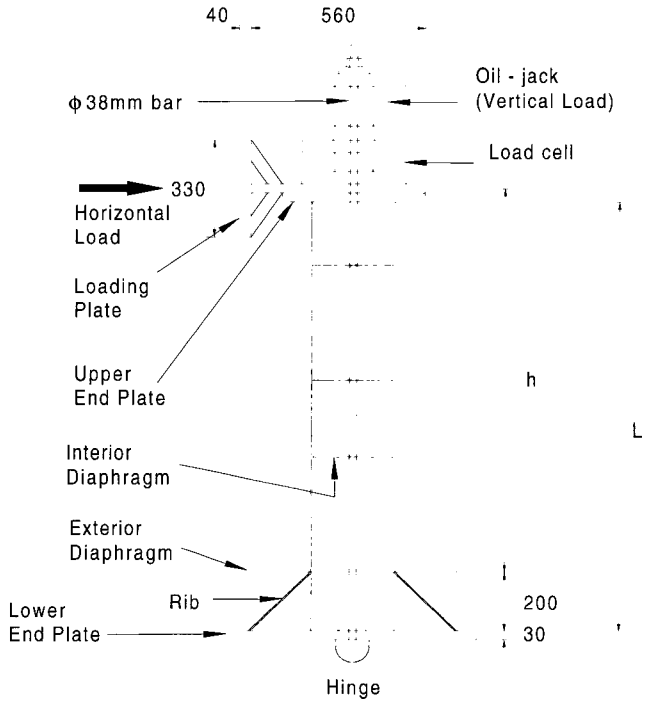

Fig. 3 Schematic drawing of test setup

The horizontal displacement history consists of sequences of fully reversed displacement cycles, the peak displacements were increased stepwise after three successive cycles at each displacement level. The lateral yield load, H_{yo} and the lateral deflection of column top corresponding to H_{yo},

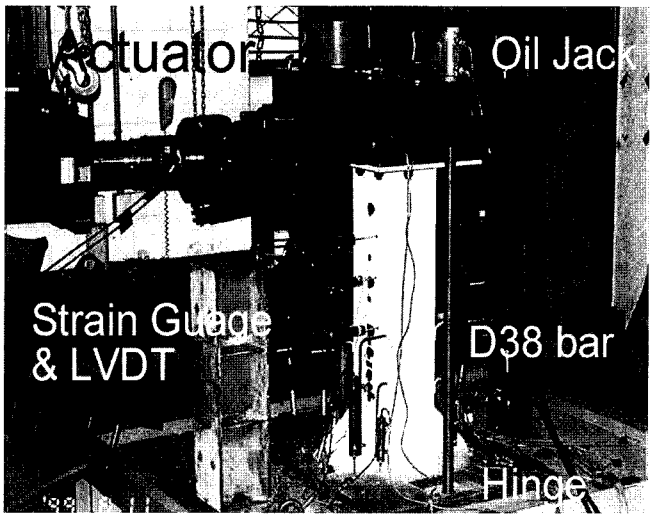

Fig. 4 Test configuration

δ_{yo} were defined as Eq. (3) and Eq. (4),

$$H_{yo} = \frac{M_y}{h} \tag{3}$$

$$\delta_{yo} = \frac{H_{yo} h^3}{3EI} \tag{4}$$

in which, M_y and I are the yield moment and the moment of inertia of the steel section, respectively.

3. Test results

3.1 Structural behavior

The concrete-filled composite columns had shown higher strength, ductility and larger energy absorption capacity than hollow steel box columns. Horizontal load versus displacement relation normalized with yield load and corresponding displacement respectively are shown in Figs. 5 (a)-(d). From the test results of S60 series specimens with varying in-filled concrete height as shown in Fig. 5(a), it can be concluded that the ultimate strength and deformation capacity were obviously improved by the filled-in concrete. As the height of filled-in concrete is increased, the strength, stiffness and deformation capacity is enhanced except the fully concrete-filled column. The maximum load and deformation capacity of fully concrete-filled columns along overall length of the specimens(l_c/h=1.0) were lower than those of the half-filled specimens(l_c/h=0.5), since they could not sustain high energy absorption that the hollow steel part above in-filled concrete of partially-filled columns had.

In order to find the effect of width-thickness ratio, the comparison of two stiffened specimens with same slenderness ratio and loading cycles, S40-25-5-3(R_f=0.41) and S60-25-5-3 (R_f=0.60), is shown in Fig. 5(b). The comparison showed that the maximum strength and ductility were decreased as the width-thickness ratio was increased. With the same filled-in concrete length and the number of the loading cycles, the maximum strength and ductility were decreased as the slenderness ratio was increased as shown in Fig. 5(c). The results of cyclic tests with three cycles at each displacement level(n=3) and monotonic tests(n=0) showed that the maximum loads were nearly the same as shown in Fig. 5(d). However, the ductility was sharply decreased after the maximum load with three cycles of loading. The number of loading cycles had large effects on the ductility rather than the strength as the resistance capacity was abruptly decreased after the maximum load.

3.2 Moment-curvature relations

3.2.1 Material properties model

The cross section analysis procedure was developed to obtain the moment-curvature relations for concrete-filled composite columns subjected to compression combined with uni-axial bending moment. The cross section analysis procedure to trace the nonlinear behavior of concrete-filled

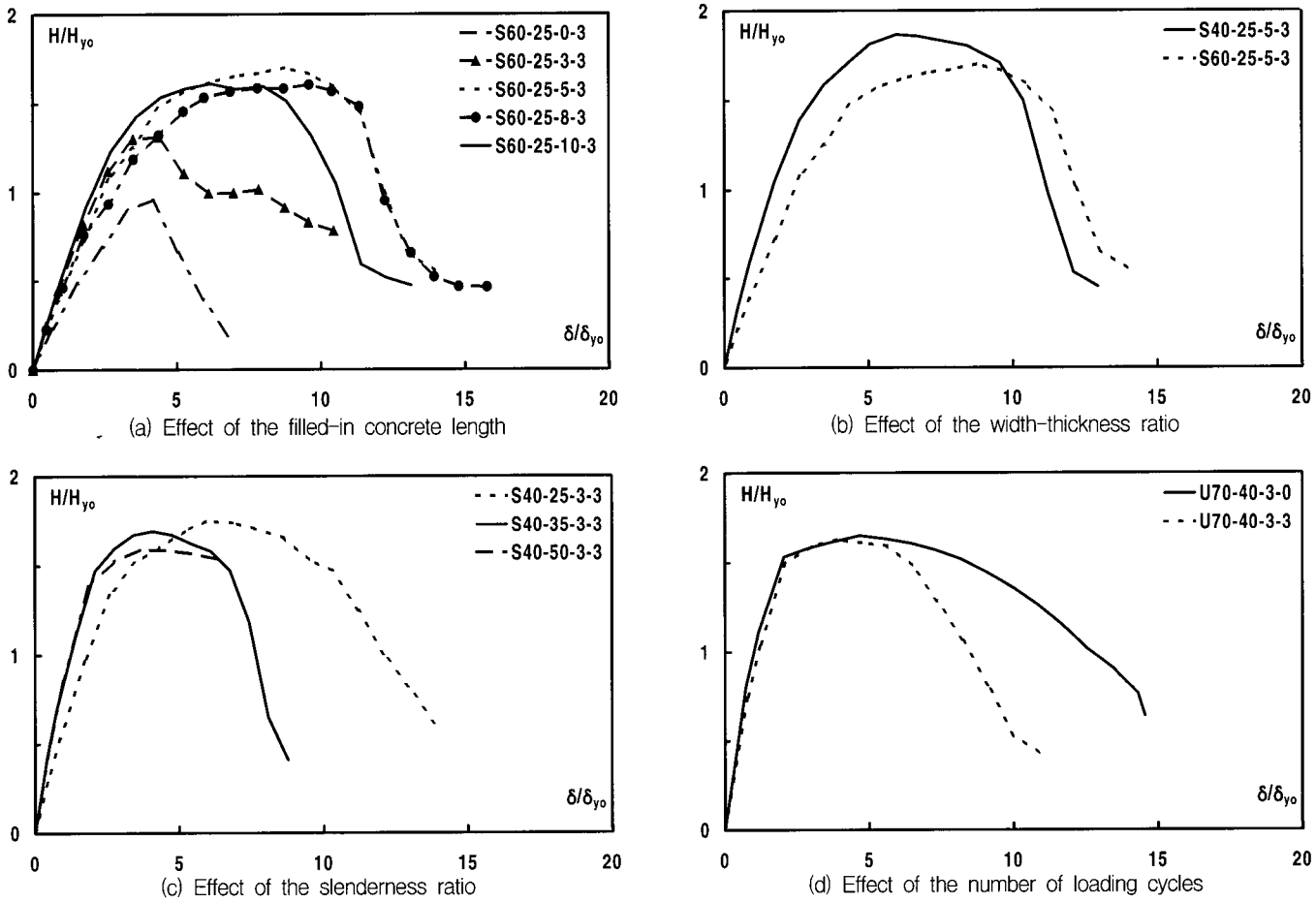

(a) Effect of the filled-in concrete length

(b) Effect of the width-thickness ratio

(c) Effect of the slenderness ratio

(d) Effect of the number of loading cycles

Fig. 5 Envelop of horizontal load-horizontal displacement curves

composite columns was able to include the nonlinear material properties of steel plate and filled-in concrete. In the procedures, it was supposed that the stress-strain relation of steel plate was bi-linear, neglecting the strain-hardening range of the properties. The stress-strain relation curves for concrete proposed by Burdtte & Hilsdrof model was assumed for the compressive strength of concrete and Lodygowski and Szumigala model was adopted for the tensile strength of concrete. Burdtte & Hilsdrof model(1972) is shown in Fig. 6 and expressed as Eq. (5)

$$f_c = f_{ck}\left[2\left(\frac{\varepsilon_c}{\varepsilon_o}\right) - \left(\frac{\varepsilon_c}{\varepsilon_o}\right)^2\right] \tag{5}$$

in which, f_{ck}=the compressive strength of concrete, ε_c =strain of concrete and ε_o=strain at f_{ck}(0.0023).

Lodygowski and Szumigala model(1992) is given in Eq. (5a)-(5c) and is shown in Fig. 7.

$$f = \frac{\varepsilon f_t}{\varepsilon_r}, \qquad \varepsilon \le \varepsilon_r \tag{6a}$$

$$f = \frac{(\varepsilon + \varepsilon_a) f_t}{\varepsilon_r - \varepsilon_a}, \qquad \varepsilon_r < \varepsilon \le \varepsilon_a \tag{6b}$$

$$f = 0, \qquad \varepsilon > \varepsilon_a \tag{6c}$$

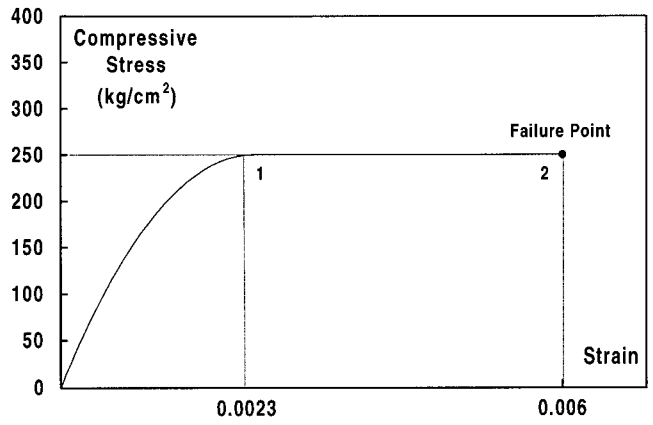

Fig. 6 Compressive stress-strain curve of concrete

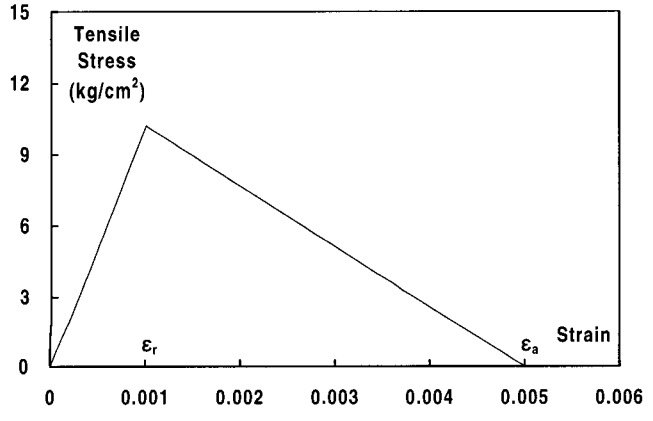

Fig. 7 Tensile stress-strain curve of concrete

in which, $f_t = (0.6\sqrt{f_{ck}} \le f_t \le 1.10\sqrt{f_{ck}})$, ε_r=strain at maximum tensile stress, ε_a=strain where the tensile stress equals zero.

3.2.2 Cross section analysis method

The cross section analysis involves the subdivision of the cross section into a large number of layers as shown in Fig. 8, to allow the strain distribution as a unique linear function. Since the slip strain between steel plate and filled-in concrete was not observed in the test, the slip strain was neglected in the analysis of composite columns. Longitudinal stiffeners and diaphragms increased the bond strength so that it could resist the slip between steel plate and filled-in concrete. Therefore the curvature is the same in steel plate and filled-in concrete.

To obtain moment-curvature relations for a given cross section, the following procedures were adopted. The strain at the top fiber was assumed. Then the neutral axis depth was assumed so that the curvature and the strain distribution were obtained. The axial force N in the section was determined from Eq. (7)

$$N = \sum_{i=1}^{n} f_i \cdot d_i \cdot b \tag{7}$$

where the stress f_i was a function of strain at the centroid of each layer, obtained by using the stress-strain relations mentioned above.

Axial force N and P were summed up to produce the axial resultant force. The method of bi-section was then used to converge on the value d_i for which the axial resultant force was zero to a given accuracy. The moment of the section was obtained by summing up the moment of the force of each layer as follows.

$$M = \int y' \cdot f \cdot dA = \Sigma f_i \cdot d_i \cdot b \cdot (y - d_n) \tag{8}$$

This procedure was repeated with increasing the strain to obtain the moment-curvature relationship. The numerical results obtained by the cross section analysis were given and compared with the test results and Usami's researches(1994).

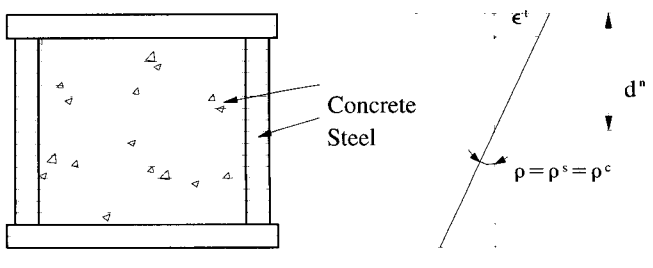

Fig. 8 Subdivision of cross section

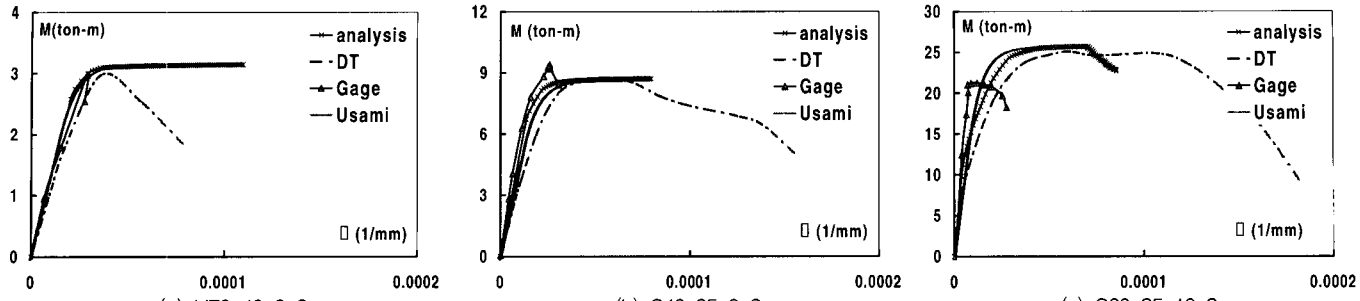

(a) U70-40-0-3 (b) S40-25-0-3 (c) S60-25-10-3

Fig. 9 Moment-curvature curves

As shown in Fig. 9, due to the local buckling of the steel plate where the linear displacement transducers(LVDT) and the strain gages were attached and axial-shortening of column due to axial compression, the moment-curvature relations between tests and numerical results did not agree well. However, the cross section analysis procedure seems to be reliable to predict the moment-curvature relation of concrete-filled composite columns at least up to the ultimate moment.

4. Ductility

4.1 Ductility factor

The ductility is one of the most important considerations in the seismic design. The design strength and the size of section can be substantially reduced if the structure has a large deformation capacity beyond the elastic limit of the material. The ductility factor for evaluating the deformation capacity could be defined as the ratio of the displacement corresponding to the maximum lateral load, δ_m, to the displacement at which first yield or local buckling occurs, δ_y and expressed as Eq. (9). However, since the collapse does not occur at the ultimate load and the degradation slope of the load-deformation curve after the peak point is very gentle, the ductility factor of Eq. (9) cannot be reasonable to define the ductility of the column.

$$\mu_m = \frac{\delta_m}{\delta_y} \tag{9}$$

where δ_y is the horizontal displacement corresponding to first yield or local buckling(horizontal displacement at the top of column corresponding to $H=H_y$) and is the horizontal displacement corresponding to $H=H_{max}$.

The failure point can be defined as the point where the crack initiates at or near the welded part in the bottom of column. Therefore, the ductility factor for deformation capacity can be expressed as Eq. (10).

$$\mu_{ci} = \frac{\delta_{ci}}{\delta_y} \tag{10}$$

where displacement δ_{ci} indicates the displacement at the moment that the initiation of cracks in the weld was observed.

On the other hand, the ductility factors μ_{95}, μ_{90} and μ_{85} can also be proposed that the failure point of the column be defined as a point where the load-carrying capacity is degraded to H_{95}, H_{90} and H_{85} respectively: 95%, 90% and 85% of the maximum load are shown in Fig. 10. Ge and Usami(1994) recommended the 95% of maximum load could be assumed to be failure point. The ductility factors above mentioned are listed up and compared in Table 3.

The displacement ductility factor obtained by using the load-displacement relations has been increased with the increment of filled-in concrete length, while it has been decreased according to the increment of width-thickness ratio, slenderness ratio and the number of loading cycles. In Table 3, it can be found that the increment of μ_{95} is larger than that of μ_m according to the strengthening effect. In this paper, the point of δ_{ci} or the point of δ_{90} can be proposed as a collapse point of the concrete-filled composite columns, whereas δ_{80} is defined as a collapse point for reinforced concrete columns.

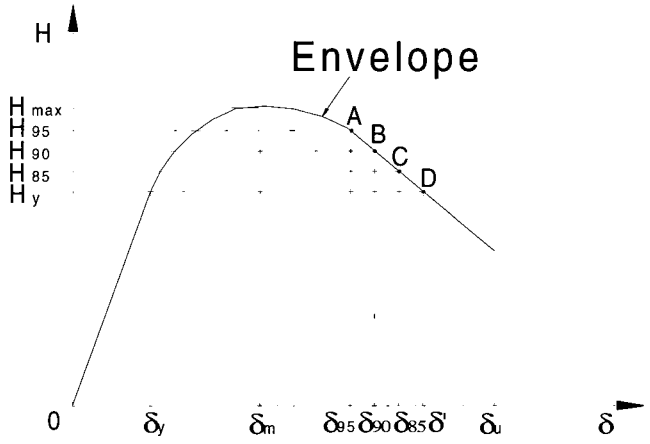

Fig. 10 Definition of collapse point

Table 3 Ductility factor

Specimens	δ_m (cm)	δ_{95} (cm)	δ_{90} (cm)	δ_{85} (cm)	δ_y (cm)	δ_{ci} (cm)	Ductility Factor				
							μ_m	μ_{95}	μ_{90}	μ_{85}	μ_{ci}
U70-40-0-3	1.33	1.72	1.85	2.02	0.55	2.65	2.42	3.13	3.36	3.67	-
U70-40-3-3	2.89	4.57	4.93	5.16	0.53	4.86	5.45	8.62	9.30	9.74	9.17
U70-40-3-0	3.50	5.47	6.50	7.17	0.47	8.76	7.45	11.64	13.83	15.26	18.64
U70-60-3-3	4.60	6.57	8.78	10.06	0.98	9.05	4.69	6.70	8.96	10.27	9.23
U90-40-0-3	1.85	2.79	2.86	2.96	0.61	2.72	3.03	4.57	4.69	4.85	-
U90-40-3-3	2.77	2.89	3.02	3.11	0.50	2.77	5.54	5.78	6.04	6.22	5.54
S40-25-0-3	2.41	2.92	3.12	3.50	0.86	4.66	2.80	3.40	3.63	4.07	-
S40-25-3-3	2.54	3.66	3.93	4.35	0.59	4.82	4.31	6.20	6.66	7.37	8.17
S40-25-5-3	2.57	3.82	4.17	4.45	0.55	3.62	4.67	6.95	7.58	8.09	6.58
S40-25-3-3(S)	2.86	3.14	3.24	3.31	0.56	3.63	5.11	5.61	5.79	5.91	6.48
S40-35-3-3	3.10	4.31	5.03	5.22	0.70	5.13	4.43	6.16	7.19	7.46	7.33
S40-50-3-3	5.53	-	-	-	1.38	-	4.01	-	-	-	-
S60-25-0-3	2.54	2.67	2.75	2.82	1.11	3.61	2.29	2.41	2.48	2.54	-
S60-25-3-3	2.66	2.92	3.00	3.16	0.67	4.78	3.97	4.36	4.48	4.71	7.13
S60-25-5-3	5.33	6.23	6.67	6.91	0.80	5.85	6.66	7.79	8.34	8.64	7.31
S60-25-8-3	5.85	6.76	6.97	7.03	0.75	6.33	7.80	9.01	9.29	9.37	8.44
S60-25-10-3	3.77	5.30	5.6	5.80	0.64	5.37	5.89	8.28	8.75	9.06	8.39

4.2 Response modification factor

The response modification factor was experimentally developed from the damage of earthquakes and the behavior characteristics in the past. The ductility should usually be considered in the seismic design of large scale or dangerous structures that are located in the severe or moderate earthquake regions. The response modification factor is conservatively used in the seismic deign in order to consider the ductility of the structural members properly in the case that first order analysis is applied.

In this paper, the response modification factor was obtained using the equivalent energy method. If the collapse point on the load-displacement curve(Fig. 11.) is defined as occurring at the maximum load point($H=H_{\max}$), the response modification factor can be obtained with Eq. (10) obtained by equating the area under the elastic curve "OAB" with that under the inelastic curve "OCDE". In the same manner, the collapse point can be defined as occurring at a point where the load-carrying capacity is deteriorated to 90%($H=H_{90}$), the response modification factor expressed in Eq. (11) can be obtained by equating the area under the elastic curve "OAB" with that under inelastic curve "OCDFG". When the collapse point is defined as the load-carrying capacity is deteriorated to 95%($H=H_{95}$), 85%($H=H_{85}$), the response modification factor was determined in the similar way

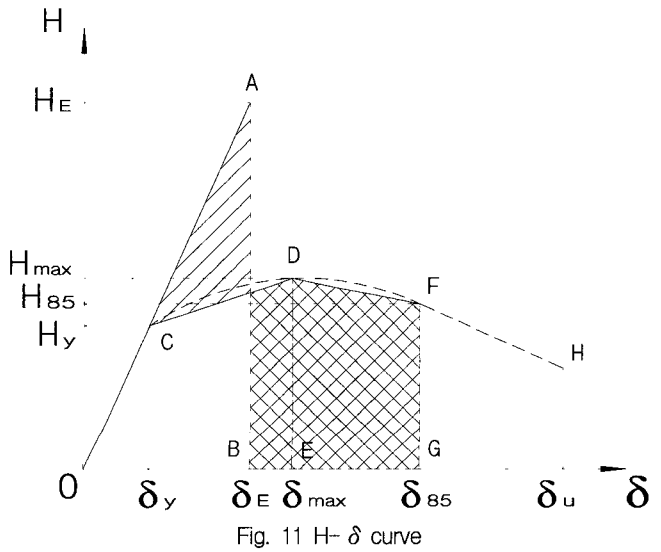

Fig. 11 H-δ curve

$$R_m=\sqrt{\mu_m(1+\alpha)-\alpha} \tag{11}$$

$$R_P=\sqrt{\mu_m(1-\beta_P)+\mu_P(\alpha+\beta_P)-\alpha} \tag{12}$$

where $\alpha=\frac{H_{\max}}{H_y}$ and $\beta_P=\frac{H_P}{H_y}=\frac{P}{100}\cdot\alpha$

in which, P=95, 90, 85.

The response modification factor calculated on the basis of initiation of crack is drawn for three important geometric factors respectively in Figs. 12(a)-(c) to inspect the effect on the response modification factor. The effect of slenderness ratio is given in Fig. 12(a). The effect was increased with the increase of the ratio up to the certain limit. The width-thickness ratio has similar effects to slenderness ratio as

shown in Fig. 12(b). The effect of filled-in concrete height on the response modification factor was also increased as the height of filled-in concrete became higher as could be seen in Fig. 12(c). The number of loading cycle had a significant effect on not only the response modification factor but also energy dissipation capacity of the composite column.

If the collapse point was defined as occurring at the 90% load point of the maximum load, i.e. $H = H_{90}$, or at the load point where the cracks occurred, the response modification factor was estimated in the range of the values from 4.4 to 6.0 except for two specimens, which can be seen in Table 4 and Figs. 12(a)-(c). However, the value of three is defined for a single column in the Korean Standard Specifications for Highway Bridges(1996), regardless of material types. The provision may be unreasonable and uneconomical for the design of bridge piers. The response modification factor could be modified in consideration of the results listed in Table 4. In this paper, it is suggested that the response modification factor should be defined as four or five for the concrete-filled composite column, if the filled-in concrete height is over 30% of column length. Moreover, if the filled-in concrete height is over 50% of column length, the response modification factor can be taken as five.

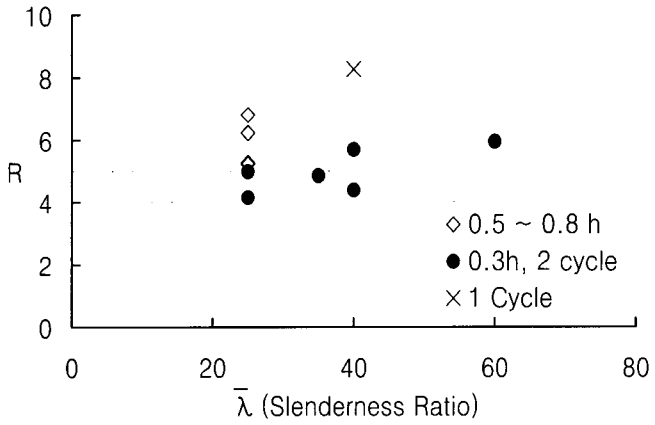

(a) R- $\bar{\lambda}$ curve

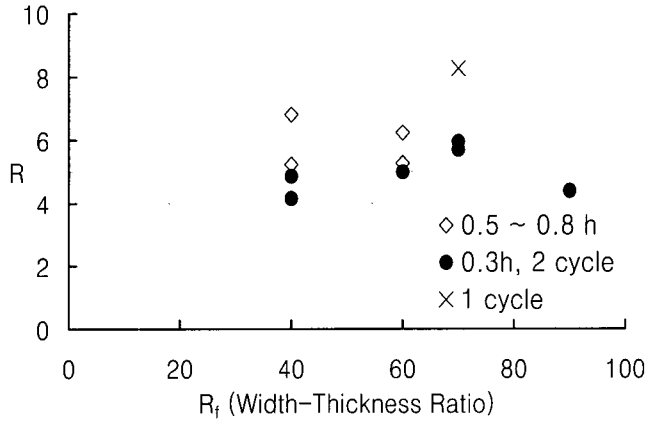

(b) R-R_f curve

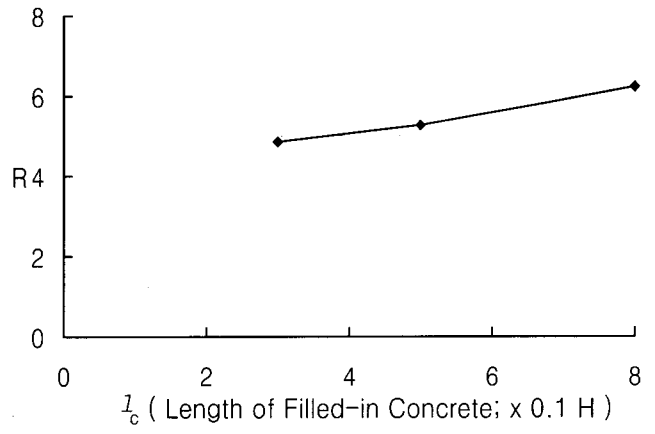

(c) R- l_c curve

Fig. 12 Response modification factor

Table 4 Response modification factor

Specimen	α	β_{95}	β_{cr}	β_{85}	β_{ci}	Response modification factor				
						R_m	R_{95}	R_{90}	R_{85}	R_{ci}
U70-40-3-3	2.32	2.20	2.09	1.97	2.16	3.97	5.49	5.72	5.85	5.70
U70-40-3-0	2.35	2.23	2.12	2.00	1.73	4.75	6.47	7.15	7.52	8.26
U70-60-3-3	2.43	2.31	2.19	2.07	2.35	3.70	4.81	5.78	6.22	5.95
U90-40-3-3	3.04	2.88	2.74	2.58	1.58	4.40	4.55	4.71	4.81	4.40
S40-25-3-3	2.19	2.08	1.97	1.86	1.89	3.40	4.43	4.62	4.89	5.23
S40-25-5-3	2.33	2.22	2.10	1.98	1.30	3.64	4.86	5.11	5.29	6.81
S40-25-3-3(S)	1.92	1.82	1.73	1.63	1.20	3.60	3.85	3.93	3.96	4.16
S40-35-3-3	2.12	2.01	1.91	1.80	1.99	3.42	4.34	4.78	4.86	4.86
S60-25-3-3	2.36	2.24	2.12	2.01	2.06	3.31	3.57	3.64	3.77	4.99
S60-25-5-3	3.06	2.91	2.75	2.60	2.71	4.90	5.54	5.81	5.93	5.27
S60-25-8-3	2.89	2.74	2.60	2.46	2.73	5.24	5.85	5.97	5.99	6.23

5. Conclusions

Concrete-filled composite columns under constant axial force and cyclic lateral loading showed generally prominent earthquake-resistance characteristics in the inelastic behavior. It was also found that the in-filled concrete could effectively improve the strength, ductility and energy absorption capacity in comparison with those of the hollow steel columns. This was resulted from that the inward local plate buckling displacements were prevented by filled-in concrete and the local buckling deformation was delayed in their initial buckling. The collapse point of concrete-filled composite columns was denoted at a point where the load-carrying capacity is reduced to 90% of the maximum load or where the crack in the steel plate or joints occurs. The ductility and energy absorption capacity were increased when the filled-in concrete length was increased. However, those were decreased as the width-thickness ratio or the slenderness ratio was increased. Since the response modification factors were ranged from 4.4 to 6.0 in the test, it was suggested that the response modification factor could be taken as

four when the filled-in concrete length exceeds 30% of column length.

A simple cross section analysis procedure has been proven to be an accurate and effective way to predict the moment-rotation relation of composite columns.

Reference

1. Ministry of Construction & Transportation, *Korean Standard Specifications for Highway Bridges*, 1996.
2. Kwon, Y. B., Song, J. Y., and Kim, S. K., "The structural behavior of concrete-filled steel pier," *Proceedings of IABSE Congress*, Lucerne, 2000. 9.
3. Ge, H. and Usami, T., "Cyclic test of concrete-filled steel box columns," *Journal of Structural Engineering*, Vol. 122, No. 10, 1996, pp. 1169-1177.
4. Chen, W. F. and Lui, E. M., *Structural Stability*, Elsevier Pty. Ltd., New York, 1996.
5. Ge, H. and Usami, T., "Development of earthquake-resistant ultimate strength design method for concrete-filled steel structures," *Research Report No. 9401*, Nagoya University, Japan.
6. Lodygowski, T. and Szumigala, M., "Engineering models for numerical analysis of composite bending members," *Mech. of Struct. and Mach.*, Vol. 20, No. 3, 1992, pp. 363-380.
7. Korean Association of Highway and Transportation, *Design Specifications for Highway Bridges*, 2000.